



Politecnico
di Bari

Repository Istituzionale dei Prodotti della Ricerca del Politecnico di Bari

Sustainability of Vanadium Redox-Flow Batteries: Benchmarking Electrolyte Synthesis Procedures

This is a pre-print of the following article

Original Citation:

Sustainability of Vanadium Redox-Flow Batteries: Benchmarking Electrolyte Synthesis Procedures / Dassisti, Michele; Cozzolino, G.; Chimienti, M.; Rizzuti, Antonino; Mastroianni, Pietro; L'Abbate, Pasqua. - In: INTERNATIONAL JOURNAL OF HYDROGEN ENERGY. - ISSN 0360-3199. - STAMPA. - 41:37(2016), pp. 16477-16488.
[10.1016/j.ijhydene.2016.05.197]

Availability:

This version is available at <http://hdl.handle.net/11589/69969> since: 2021-03-31

Published version

DOI:10.1016/j.ijhydene.2016.05.197

Terms of use:

(Article begins on next page)

Sustainability of Vanadium Redox-Flow Batteries: benchmarking Electrolyte Synthesis Procedures.

M. Dassisti a, G. Cozzolino b, M. Chimienti b, A. Rizzuti c, *, P. Mastrorilli c, P. Labbate c

a Dipartimento di Meccanica, Management e Matematica, Politecnico di Bari, Bari, Italy.

b InResLab, Monopoli (Bari), Italy.

c Dipartimento di Ingegneria Civile, Ambientale, del Territorio, Edile e di Chimica, Politecnico di Bari, Bari, Italy.

* Corresponding author. E-mail address: a.rizzuti@poliba.it.

Abstract

This work focuses on the assessment, in terms of effectiveness, feasibility and sustainability, of three different synthetic procedures for the synthesis of a vanadium-based mixed-acid electrolytes that can to be used in an any kind of vanadium redox-flow battery batteries (VRFBs). Procedures considered consisted in: a) the mere mixing of suitable vanadium precursors (Electrolyte A); b) the chemical reduction of V2O5 by oxalic acid (Electrolyte B); c) the electrochemical reduction of V2O5 using a home-made “H-shaped” electrolysis cell (Electrolyte C). VRFB properties such as energy efficiency, mean charge-discharge voltages, cycle duration, cut-off voltage, as well as stability and conductivity of the electrolyte were analyzed and compared with the state-of-the-art. Measurement procedures adopted were Experimental tests carried out on a laboratory scale VRFB battery comprised: thermal stability test, cyclic voltammetry, electrochemical impedance spectroscopy measurements and charge-discharge tests on a laboratory scale VRFB battery. A Life Cycle Assessment of the three electrolytes is also presented for benchmarking purposes.

Keywords: Storage systems; Vanadium redox-flow battery; electrochemical reduction, LCA, sustainability,

1. Introduction

The first Vanadium Redox Flow Battery (VRFB) concept was conceived in 1975 at the US National Aeronautics and Space Administration (NASA) [1,2]. Nowadays, redox flow battery is considered one of the most promising technologies as electrochemical energy storage system, due to independence of energy and power rating, fast response, ambient temperature operation, and extremely long life. In particular, VRFB has an additional advantage in that it does not suffer from permanent self-discharge thanks to the use of the same element in both cell compartments. VRFB possesses the proper technology maturity for market uptake in the next years and several VRFB systems are already demonstrated all over the world [3-8].

Although VRFB is one of the more consolidated technologies among the flow type batteries, it has great margins of technological improvements and developments for the fabrication of short-term and long-term storage devices [9]. This technology possesses an extraordinary operational flexibility, as it is suitable to operate in combination to a wide range of renewable and conventional energy application [10,11]. Because of the intrinsic intermittent nature of the renewable energy sources (RES), VRFB may represent an efficient tool for the requalification of the energy provided to the grid [9,12,13], to confirm the

use of renewable energy [10,14], to enhance Smart Grid [151] and to implement Stand Alone Power Supply (SAPS) system for off-grid applications [11,14]. A recent work assesses the use of fast charging stations for Electric Vehicles in conjunction with VRFBs [16].

The main VRFB drawback of VRFB is its high capital cost, which is one of the major limitations to market uptake and widespread deployment of such systems. The high capital cost of VRFB is due to several factors such as the use of expensive vanadium precursors, costly Nafion® membranes [1217-19]], and the use of additional electrolyte temperature management system in order to prevent precipitation of vanadium compounds, when a conventional supporting pure sulphate electrolyte is used [88].

In order to break market barrier, beside the optimization of the cell and stack design [20] it is necessary to reduce the VRFB overall cost, paying great attention to the cost of vanadium electrolyte being , which accounts, approximately, for the 40-45% of the total [2113]. The laboratory methods for vanadium electrolyte preparation require either the use of expensive vanadium compounds (VOSO₄, V₂O₃, or VC₁₃) [1422,1523], and chemical reducing agent (typically oxalic acid or ethylene glycol), or tricky multi-step processes, to dissolve divanadium pentoxide (i.e. the raw material) in the supporting electrolyte. Others methodologies focus on the implementation of relatively complex processes and/or on the use of expensive stabilizing agents, to produce a conventional pure sulphate vanadium electrolyte (in which sulphuric acid is the support electrolyte) [1624-1927], having a lower performance with respect to a mixed acid supporting vanadium electrolyte (in which the support electrolyte is made up of sulphuric acid and hydrochloric acids) [1523].

Life Cycle Assessment (LCA) investigates environmental impacts of systems or products from cradle to grave throughout the full life cycle, from the exploration and supply of materials and fuels, to the production and operation of the investigated objects, to their disposal/recycling. Few LCA studies have been performed for redox flow batteries so far. A comparison has been reported between a big size VRFB and a Lead-Acid Battery systems [28]. However, still strong uncertainties affected such LCA analysis, since two different stages of technology maturity are compared (contrary to Lead-Acid Batteries, VRFBs are even today far from being a largely industrialised systems).

In this work, three preparation methods of mixed acid vanadium electrolyte electrolytes for VRFB were compared in terms of effectiveness, feasibility and sustainability. The first method consists in the mere mixing of suitable vanadium precursors affording Electrolyte A. The second method requires the chemical reduction of V₂O₅ by oxalic acid and produces Electrolyte B. The third method, yielding Electrolyte C, consists in the electrochemical reduction of V₂O₅ using a home-made "H-shaped" electrolysis cell. The electrolyte properties (i.e. stability, energy density, etc.) were analysed in dependence in function of of the electrolyte production methods. For To this purpose, thermal stability tests as well as Cyclic Voltammetry (CV) and Electrochemical Impedance Spectroscopy (EIS) measurements were performed. The performances of laboratory scale VRFB using the three different electrolyte produced were evaluated by means of several consecutive charge-discharge cycles. The work was completed with an environmental sustainability study performed by the Life Cycle Assessment (LCA).

2. Experimental

2.1. Materials

V205 (provided from Duferco Energia spa, 99.95%), VOSO₄·2H₂O (Sigma-Aldrich, 97%), VCl₃ (Sigma-Aldrich, 99.999%), HCl (Sigma-Aldrich, 37%wt, d = 1.20 g/mL) , H₂SO₄ (Sigma-Aldrich, 98%wt, d = 1.84 g/mL) and C₂H₂O₄·2H₂O (Sigma-Aldrich, 99.6%) were used as received.

2.1.1. General procedure for preparation of Electrolyte A. In a 2.0 L graduated round flask, 55.5 mL (1.0 mol) of H₂SO₄ was added to 450.0 mL of deionized water at 298 K. The dissolution of the concentrated acid in deionized water is strongly exothermic and, then, after letting the sulphuric acid solution to cool down to 298 K, 164.2 mL (2.0 mol) of HCl was added. Then, 205.155 g (1.0 mol) of VOSO₄·2H₂O and 162.165 g (1.0 mol) of VCl₃ were added to the mixed acid solution and deionised water was poured to the flask to reach the total volume of 1.0 L. The as-prepared electrolyte solution was magnetically stirred for 3 h, obtaining the V³⁺/V²⁺ working electrolyte with a [V³⁺]/[V²⁺] ratio equal to 1.0. UV-Vis: [V³⁺] = 1.045 06 M; [V²⁺] = 1.034 03 M. Potentiometric precipitation titration: [Cl⁻] = 4.97 M.

2.1.2. General procedure for preparation of Electrolyte B. In a 2.0 L graduated round flask, 111.0 mL (2.0 mol) of H₂SO₄ was added to 450.0 mL of deionized water at 298 K. After cooling of sulphuric acid solution, 410.5 mL (5.0 mol) of HCl was added for the preparation of the mixed acid electrolyte support. Then, 126.63 g (1.0 mol) of oxalic acid dihydrate (C₂H₂O₄·2H₂O), and 182.80 g (1.0 mol) of vanadium pentoxide (V₂O₅) were added and deionised water was poured to reach the total volume of 910 mL. The reaction mixture was magnetically stirred for 96 h, during which 90 mL of water were produced. After reaction, the electrolyte was filtered by means of a 50 µm glass frit to remove a gelatinous precipitate which formed during reaction. After filtration, the as-obtained V²⁺ solution (Electrolyte D) was electrolysed in a flow cell to reduce half of the V(IV) to V(III). Each half-cell reservoir was filled with 125 mL of the electrolyte which was cyclically pumped into the corresponding half-cell by dual head peristaltic pump with a flow rate corresponding to an electrode face velocity of 2 cm s⁻¹. Each electrolyte solution was charged galvanostatically at a current density of 20 mA cm⁻² up until to reach a the cell potential of reached the value of 1.9 V, in order to produce V³⁺ and V²⁺ in the negative and the positive compartment, respectively. At the end of the electrolysis, 125 mL of the catholyte was mixed with 125 mL of fresh Electrolyte D (containing V²⁺ in H₂SO₄/HCl) obtaining a working electrolyte having a [V³⁺]/[V²⁺] ratio equal to 1 referred to as Electrolyte B. UV-Vis: [V³⁺] = 0.990 M; [V²⁺] = 1.025 03 M. Potentiometric precipitation titration: [Cl⁻] = 4.93 M.

2.1.3. General procedure for preparation of Electrolyte C. This process consisted in the dissolution assisted by an electrochemical reduction of divanadium pentoxide in mixed acid solution. The electrolysis cell was a home-made H-shaped cell having half-cell compartments with a volume of 2.0 L (10 cm x 10 cm x 20 cm). The half-cell compartments were interconnected each other by means of a horizontal duct (s = 7.5 cm, l = 10 cm). A cationic exchange membrane (Nafion® 115) was housed in the middle of the horizontal duct. The membrane assured mass and charge transfer as well as hydraulic separation between the half-cell. The electrolysis cell was equipped with a SGL GDA 3 EA carbon felt electrode (geometric area = 300 cm²) at the acting as negative compartment where the conductive connection with the current generator was assured by a platinum joint; the positive side of the cell was equipped with a

platinum wire electrode ($s = 0.05$ cm, $l = 20$ cm,). Each compartment of the H-shaped electrolysis cell were was filled with a fixed volume of 1.0 L of a mixed acid supporting electrolyte solution made up of 2.0 M H₂SO₄ and 5.0 M HCl. Then, 182.80 g (1.0 mol) of V2O5 powder was added only into the negative cell compartment and electrochemically reduced under vigorous magnetic stirring until the $[V^{3+}]/[VO_2^+]$ ratio became exactly 1.0 (electrolysis time = 96 h). This V³⁺/VO₂⁺ working electrolyte was referred to as Electrolyte C. UV-Vis: $[V^{3+}] = 0.8304$ M; $[VO_2^+] = 0.8505$ M. Potentiometric precipitation titration: $[Cl^-] = 4.02$ M.

2.2. Methods

2.2.1. Instrumentation. UV-Vis analyses were carried out using a JASCO V670 instrument. Potentiometric analyses were performed by means of a Metrohm Titrino instrument. Cyclic voltammetry (CV) measurements were performed with a potentiostat Autolab-PGSTAT302N. Electrochemical Impedance Spectroscopy measurements were performed with a potentiostat Autolab PGSTAT302N-FRA32M equipped with an AC impedance module.

2.2.2. Electrolyte composition and chloride concentration measurements.

Electrolyte composition was evaluated by means of UV-Vis spectroscopy measurement performed on 1:100 diluted starting electrolyte solutions in the wavelength range 300-900 nm. The total chloride ions concentration present in the electrolyte solutions was assessed by means of a potentiometric titration method using 0.010 M AgNO₃ aqueous solution as titrant. Before the analysis, the electrolyte solution was diluted 10000 times. 50 mL of the diluted electrolyte solution added with 2.0 mL of 2.0 M HNO₃ aqueous solution was used as sample for the chloride determination.

2.2.3. Electrolyte thermal stability test. The thermal stability of Electrolytes A-C was checked. Each solution sample (~10 mL) was sealed in a PTFE sampling tube and then immersed in a thermos-cryostat without stirring. The samples were monitored twice a day by means of UV-Vis spectroscopy to register the total vanadium concentration. The stability tests were carried out at -5, 0, 25 and 55 °C. After 15 days, none of the Electrolytes A-C suffered from precipitation [1321] and the total vanadium concentration remained equal to the initial value.

2.2.4. CV and EIS measurements. Cyclic voltammetry experiments were carried out under pure dinitrogen, using a 20 mL electrochemical cell equipped with carbon felt rod (diameter 6 mm, height 5 mm, bulk density 0.09 g cm⁻³, area weight 425 g cm⁻²) as working electrode, and glassy carbon (diameter 3 mm) as counter electrode, and saturated calomel as reference electrode. In order to determine the cell high-frequency response, EIS measurements were performed on the laboratory scale VRFB at a state of charge of 80 % corresponding to an open circuit potential (OCP) of 1.4 V. The frequency ranged from 100 kHz to 0.05 Hz with sinusoidal excitation voltage of 5 mV. The tests were carried out without electrolyte flow in order to minimize measuring errors due to mass transport process.

2.2.5 Set up of the laboratory scale VRFB. Fig. 1 shows a picture of the laboratory scale VRFB along with a sketch of its components. Both halves of the cell are constituted by a compression plate, a current collector, a graphite plate provided with holes, which constitute the flow frame, and a carbon felt electrode.

Fig. 1. (a) Lab-scale VRFB cell and (b) cell design.

The carbon felt electrode latter is positioned in the centre middle of a spacer, which is finally connected to the membrane. The tightness sealing of the system was ensured by two gasket for each half-cell (see Fig. 1b). The compression plate, acting as cell terminal plate, was made up of a 13 × 13 × 3 cm plate of PEEK polymer. The cell was fabricated by interposing a cationic exchange membrane (Nafion® 115) between two porous and layered carbon felt electrodes (5 cm × 5 cm). A flow-through configuration was adopted for the cell set-up. In fact, the graphite plate acted as a current collector while ensuring the electrolyte flow distribution through the half-cell carbon felts. A smart sealing and spacing system, constituted by a Viton gasket and a PTFE spacer arranged alternately, was used to define the compression ratio of carbon electrode, by varying the spacer and the felt thickness, respectively. SGL GFA3 EA carbon felt electrodes with a compression ratio of 0.3 was chosen for the tests. Before tests, the carbon felt was electrochemically oxidized to enhance its electrochemical activity and hydrophilicity. Two aluminium nickel coated plates acted as current collectors. The electrolyte was stored in 250 mL detached-glass reservoir for each half-cell, under nitrogen atmosphere. The electrolyte volume was 125 mL for both positive and negative reservoirs. The electrolyte was circulated through the cell compartment by means of a dual-head peristaltic pump equipped with Tygon® tubes at volumetric flow rate of 180 mL min⁻¹ corresponding to a linear electrode face velocity of 2 cm·s⁻¹. The system was purged by nitrogen and sealed prior to charge/discharge cycling to prevent oxidation of active specie (in particular V²⁺) by air in the negative compartment. For each test condition, VRFB charge-discharge curves were acquired using a battery analyser (MTI BST8-3). The flow battery was cycled between 1.9 V and 0.7 V, that represent respectively the charge and discharge cut-off voltage values at constant current density of 20 mA·cm⁻², respectively. The electrolyte flow rate was kept constant during tests. For each test condition the energy efficiency, the mean charge-discharge voltages, and cycle duration, were measured.

2.3. LCA Methodology

The adopted LCA method followed the ISO 14040: 2006 ,[2029], ISO 14044: 2006 [2130] and included four phases: determination of goal and scope, inputs and outputs Life Cycle Inventory analysis (LCI), environmental Life Cycle Impact Assessment (LCIA), and results interpretation of results [2029-2332].

2.3.1. Goal and Scope of the analysis. The goal was the comparison of the three synthetic methods used for the production of Electrolytes A-C, in order to calculate assess the environmental impacts and the corresponding indicators of the environmental sustainability. The selected functional unit (FU) was: six litres of electrolyte produced in the laboratory. As to the scope and the system boundaries, it was considered the following delimitation of the field of study: "cradle to gate". It includes all phases up to the exit article from production ("laboratory gate"), as this is the end point of the ability of researchers to directly influence the impact.

2.3.2. Inputs and outputs inventory analysis (LCI). The considered raw materials were the reagents used for the three syntheses as described in the "Materials" section. The raw materials excluded from the analysis were all those

the non-consumable ones, that is i.e. the materials of the electrolytic cells, laboratory glassware, electrodes, pumps and magnetic stirrers. The transport of the reagents was calculated as the distance from the place of purchase purposes to the place of electrolyte preparation. All reagents came from Northern Italy with the exception of deionized water (in in-house production) and V205 (which came from South Africa). Energy data: Italian energy mix was used for the magnetic stirrer (Electrolyte A, Electrolyte B, Electrolyte C), reaction energy (Electrolyte B, Electrolyte C), energy conversion (Electrolyte A), energy hydraulic system (Electrolyte A, Electrolyte B, Electrolyte C). Not all packaging and storage containers were considered.

2.3.3. Impact categories (LCIA). The method used to describe the environmental impacts of the life cycle from cradle to gate of the three methods of synthesis of the electrolyte was ReCiPe 2008 [2433]. The overall structure of the method is shown in Fig. 2. The ReCiPe method, transforms the list of Life Cycle Inventory results, into a limited number of indicator scores. These indicator scores express the relative severity on an environmental impact category. This method has the ability to evaluate 18 different categories of impact (midpoint) that can be later be converted and aggregated in three categories of environmental damage: damage on human health, damage to the quality of the ecosystem, resource depletion (endpoint) [2534,2635]. The impact categories and categories of damage have different units of measure (Disability Adjusted Life Year, Species per year, Surplus cost). To compare them, the method performs an Ecopoint conversion using the model of "Cultural Theory" proposed by Thompson in 1990 [36] bringing together the various sources of uncertainty of various choices in a limited number of prospects.

The three perspectives are: Individualist (short term, optimism that technology can avoid many problems in future), Hierarchic (consensus model, as often encountered in scientific models, this is often considered to be the default model), Egalitarian (long term based on precautionary principle thinking). In this case, the version of "Individualistic" (I) with European standardization and average weighting (version I/A) has been chosen. The used software was CMLCA (by CML, University of Leiden) and the employed database was Ecoinvent 2010 [2130].

This method allows to evaluate 18 different categories of impact (midpoint) that can later be converted and aggregated in three categories of environmental damage: damage on human health, damage to the quality of the ecosystem, resource depletion (endpoint) [25,26]. The impact categories and damage categories, have different units of measure (Disability Adjusted Life Year, Species per year, Surplus cost). The method adopted performs an Ecopoint conversion using the model of "Cultural Theory" proposed by Thompson in 1990, bringing the various sources of uncertainty in various choices in a limited number of prospects.

The three perspectives are: Individualist (short term, optimism that technology can avoid many problems in future), Hierarchic (consensus model, as often encountered in scientific models, this is often considered to be the default model) and Egalitarian (long term based on precautionary principle thinking). In our case, the version of "Individualistic" (I) with European standardization and average weighting (version I/A) has been chosen. The used software was CMLCA (by CML, University of Leiden) and the employed database was Ecoinvent 2010 [21].

Fig. 2. Relationship between LCI parameters (left), midpoint indicators (middle) and endpoint indicators (right) in ReCiPe 2008, source Goedkoop et al. [2433].

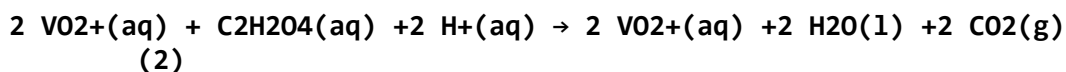
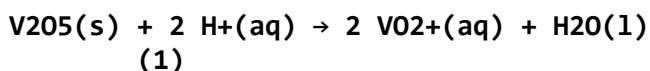
3. Results and discussion

3.1. Description of the synthetic methods for the preparation of the vanadium electrolyte

The vanadium mixed acid Electrolytes A-C were prepared using an aqueous solution of sulfuric and hydrochloric acid as supporting electrolyte and with the following theoretical concentrations: $[V^{3+}] = [VO^{2+}] = 1.0 \text{ M}$; $[SO_4^{2-}] = 2.0 \text{ M}$; $[Cl^-] = 5.0 \text{ M}$. The $[V^{3+}]/[VO^{2+}]$ ratio fixed to 1.0 allowed us to fill the cathodic and the anodic reservoirs with the same electrolyte volume during the battery start-up phase. At the end of the first system charge (i.e. electrolyte conditioning phase) the working electrolyte contained V^{2+} in the negative compartment and VO^{2+} in the positive compartments. V^{2+} and VO^{2+} were transformed into V^{3+} and VO^{2+} , respectively, after the discharge process, so to become available for a new charge-discharge cycle.

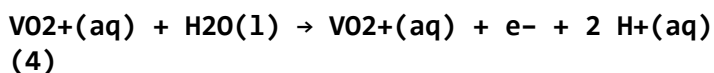
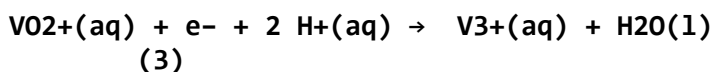
Electrolyte A was prepared by dissolution of $VOSO_4 \cdot 2H_2O$ and VCl_3 as vanadium precursors in a mixed aqueous acid solution based on containing H_2SO_4 and HCl . This method was chosen as the reference method, because it ensures a one-pot electrolyte production with controllable and repeatable properties.

Electrolyte B was prepared starting from V_2O_5 as vanadium precursor via reactions (1) and (2) consisting, the first of the dissolution of V_2O_5 and, the second, of an oxalic acid promoted reduction carried out at 298 K in a mixed aqueous acid solution composed by containing H_2SO_4 and HCl in a 2:5 molar ratio.



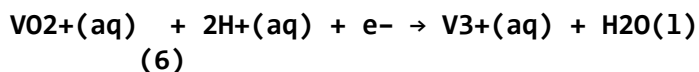
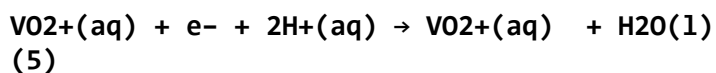
The choice of oxalic acid as a reducing agent was dictated suggested by its relatively low cost and by the full compatibility of the reaction products with the electrolytic solution. In fact, during the VO^{2+} to VO^{2+} reduction, the only secondary products are the volatile CO_2 and the benign H_2O .

The as-prepared VO^{2+} electrolyte solution was electrochemically treated by means of electrolyzed in a the flow cell to give two equal volumes of V^{3+} and VO^{2+} solutions in the negative and positive compartments, respectively, according to the following reduction and oxidation semi reactions:

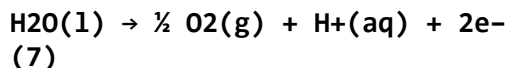


Then, by the mixing of the as-obtained V^{3+} solution with an equal volume of VO^{2+} fresh electrolyte solution, the V^{3+}/VO^{2+} working electrolyte with a $[V^{3+}]/[VO^{2+}]$ ratio equal to 1.0, was prepared achieved.

Electrolyte C preparation was carried out in an H-shaped cell and consisted of the electrolysis of a saturated solution of V_2O_5 which was stopped as soon as the concentrations of the obtained $[VO^{2+}]$ and $[V^{3+}]$ were equal. The steps by which the process proceeded are: dissolution of V_2O_5 to give VO^{2+} (react. 1); electrochemical reduction of VO^{2+} to VO^{2+} (react. 5); electrochemical reduction of VO^{2+} to V^{3+} (react. 6).



While reactions (5) and (6) proceed in the negative half-cell, water oxidation takes place in the positive compartment of the electrolysis cell (react. 7).



During the process, for each mole of electrons passing in the circuit a mole of protons migrates from the positive to the negative compartment of the H-shaped cell through the Nafion® membrane. Rearranging Faraday's law:

$$t = V \cdot [\text{V}_{\text{tot}}] \cdot n \cdot F / I$$

where t is the electrolysis time; V is the volume of reacting solution; $[\text{V}_{\text{tot}}]$ is the total vanadium concentration, I is the applied current, n is the number of electrons involved in the reaction, and F is the Faraday constant (96485 C/mol). The theoretical reaction time to obtain a final electrolyte composition of $[\text{V}^{3+}] = [\text{VO}_2^+] = 1.0 \text{ M}$ applying a constant current of 1.0 A is 80 h. The experimental value of the time needed to achieve Electrolyte C was 96 h with a process efficiency of ca. 83%.

3.2. Composition determination Chemical composition of the electrolytes UV-Visible spectroscopy was used to determine the total concentration and the speciation of vanadium in the electrolytes object of this study. Standard solutions were prepared by dissolving V^{3+} (as VCl_3) and VO_2^+ (as $\text{VOSO}_4 \cdot 4\text{H}_2\text{O}$) in $\text{H}_2\text{SO}_4:\text{HCl}$ mixed acid (2:5 mol/mol).

VO_2^+ showed absorptions at 767 nm ($\epsilon_{767\text{nm}} = 16.74 \text{ cm}^{-1} \text{ mol}^{-1} \text{ L}^{-1}$) and 650 nm ($\epsilon_{650\text{nm}} = 9.11 \text{ cm}^{-1} \text{ mol}^{-1} \text{ L}^{-1}$). V^{3+} showed a strong band at 600 nm ($\epsilon_{600\text{nm}} = 5.36 \text{ cm}^{-1} \text{ mol}^{-1} \text{ L}^{-1}$) and an absorption at 400 nm ($\epsilon_{400\text{nm}} = 8.14 \text{ cm}^{-1} \text{ mol}^{-1} \text{ L}^{-1}$), in a region in which the other V species do not absorb. Fig. 3 shows the curves for Electrolytes A-C, prepared starting from having a total mass of vanadium equal to of 2.0 mol and with the aim of having $\text{V}^{3+}/\text{VO}_2^+$ molar ratios of of 1.0. Reference to the Lambert-Beer law was adopted used to evaluate assess the following data features: Electrolyte A contained V^{3+} and VO_2^+ ions in a 1.02 ± 0.27 molar ratio and with a total vanadium concentration of $2.09 \pm 0.28 \text{ M}$; Electrolyte B contained V^{3+} and VO_2^+ ions in a 0.96 ± 0.22 molar ratio and with a total vanadium concentration of $2.02 \pm 0.28 \text{ M}$; Electrolyte C contained V^{3+} and VO_2^+ ions in a 1.03 ± 0.29 molar ratio and with a total vanadium concentration of $1.68 \pm 0.24 \text{ M}$ (Table 1).

Fig. 3. UV-Vis spectra of Electrolytes A-C.

It is worth noting that the total vanadium concentration in Electrolyte C results lower than Electrolytes A and B, due to the water produced during the electrolytic process followed for the preparation of Electrolyte C. The chloride concentration of Electrolytes A-C is also reported in Table 1. The results showed that electrolyte A and B had a total chloride concentration of

4.97±0.40 M and 4.93±0.38 M respectively, thus respecting meeting the desired target of HCl concentration (5.0 M). As expected, Electrolyte C showed a total chloride concentration of about 4.02±0.33 M, slightly lower than with respect to Electrolytes A and B. The found value of [Cl⁻] in Electrolyte C indicates that negligible (if any) chloride loss in the form of gaseous hydrochloric acid occurs during the synthesis. As a result of water dilution, Electrolyte C showed also a lower viscosity as well as a lower ionic strength than Electrolytes A and B.

Table I1

3.3. Thermal stability of the electrolytes

No precipitation was observed for all of the Electrolytes A-C over the fixed time period (15 days) in the temperature range from -5 to 55 °C. The thermal stability observed in our mixed aqueous acid solution is in accordance with previous reports [27],[1422,1523,37] claiming that the formation of species such as [V₂O₃·4H₂O]⁴⁺ or [V₂O₃Cl·3H₂O]³⁺ are responsible for the lack of precipitation over the considered temperature range considered. In Table 2 the thermal stabilities of Electrolytes A-C are compared with literature data [22, 38].

Table 2

3.4. Cyclic Voltammetry

The electrochemical behaviour was investigated at room temperature by using the three electrode system on an electrochemical apparatus. The potential range of the CV curves was 0.7÷-1.2 V. Fig. 4 displays the CV curves at a scan rate of 10 mV s⁻¹ of VO₂⁺ electrolytes obtained according to the above reported methods A, B, and C respectively. For the given scan rate of 10 mV s⁻¹, both the magnitude of the anodic peak and the cathodic peak current of the VO₂⁺/VO₂⁺ couple, as function of reduction-oxidation potential were reported. The curves were similar to each other in shape, and exhibited evidently only one couple of redox peaks.

Fig. 4. CVs of VO₂⁺ species in mixed acid solutions prepared according to the methods A-C; carbon felt (working electrode), glassy carbon (counter electrode), calomel (reference electrode), scan rate of = 10 mV s⁻¹.

In order to investigate the influence of the electrode polarization and reaction reversibility, as function of the electrolyte preparation methods, the separation difference of peak potentials, ΔE_p, and the ratio of peak current intensities of the oxidization peak (I_{pa}) to the reduction peak (I_{pc}), I_{pa}/I_{pc}, obtained from the CV measurements are summarized in Table 2.

Table 23

The results showed that Electrolyte C exhibited the best electrochemical behaviour, with the lower peak current compared to A and B electrolytes A and B respectively. Furthermore, in the case of Electrolyte C reaction kinetic results more reversible as supported from the lower value of the peak potential separations of the VO₂⁺/VO₂⁺ redox couple. The values of ΔE_p for varying from 220 mV for Electrolytes A and B were 220 mV to and 195 203 mV, passing from Electrolyte A to, respectively, with a ΔE_p Electrolyte C. value for Electrolytes B of 195 mV (Table 2). A potential difference between the oxidation peak and the reduction peak of 195 mV indicates the a quasi-reversibility of the

V02+/V02+ reaction on the carbon-felt electrode (SGL GFD5 EA). The anodic peak current to cathodic peak current ratios (I_{pa}/I_{pc}) and the peak potential separation for the V02+/V02+ redox reaction decreased on passing from Electrolyte A to Electrolyte C, demonstrating that electrolyte C showed the best redox reversibility of the V02+/V02+.+ transformation.

3.5. Electrochemical Impedance Spectroscopy

EIS is a powerful tool to identify the components (i.e. electrodes, electrolyte, membrane etc.) affecting battery performance by means of the analysis of equivalent electric circuit of the cell. Fig. 5 shows the Nyquist plots for Electrolytes A-C obtained using a charged battery filled with the desired electrolyte, at an OCP of 1.4 V, without in the absence of electrolyte flow.

Fig. 5. Nyquist plot of EIS - impedance data, at an OCP of 1.4 V, obtained by varying the electrolyte preparation methods.

Each of the three Nyquist plots is constituted by a well-defined semicircle part, in the high frequency range, followed by a linear part, in the low frequency range. This indicates that the whole impedance is determined by both charge transfer and mass transport together [1826,1927,2838]. From theoretical considerations of the chemical reactions, the setup of the battery, especially the macro-porous carbon felt electrodes and the results of the measurements, a simple equivalent circuit based on an modified Randles-circuit has been developed to describe the battery. The radius of the semicircle in the high frequency range gave the charge transfer resistance while the slope of the line in the low frequency range permits to establish that the process is driven by ion diffusion through the solution. The proposed model of the equivalent electric circuit of the cell, shown in the inset of Fig. 5, was selected with only one time constant. The rationale behind this choice is the dominance of one velocity determining chemical reaction, depending from on elements R_s (ohmic resistance), R_{ct} (the charge transfer resistance across electrode/solution interface), the Warburg diffusion and constant-phase-elements (CPE, (which describes the electrochemical double layer).

The impedance of the cell is given by the following equation:

$$Z(\omega) = R_s + (R_{ct} + 1/(Y_0, W(j\omega)^{1/2})) / (1 + Y_0, CPE(j\omega)^n (R_{ct} + 1/(1/(Y_0, W(j\omega)^{1/2})))$$

The impedance parameters obtained by fitting the experimental data are shown in Table 3, It is apparent that Electrolyte A was endowed with the lowest composed resistance R_s in comparison with Electrolytes B and C.

Table 34

As expected on the basis of the different viscosity, Electrolyte C exhibited a lower value of charge-transfer resistance R_{ct} which implies a faster charge transfer reaction kinetic at the electrolyte/electrode interface [2940], with respect to Electrolytes A-B.

CPE and W values are of the same order of magnitude for Electrolytes A-C.

3.6. Charge-discharge tests

The charge-discharge tests were performed using the monopolar cell described in the experimental part with the same operative configuration and condition. The

charge-discharge profiles are reported in Fig. 6.

The system using Electrolyte A showed a charge-discharge efficiency of 92.5% and mean charge and discharge voltage values of 1.56 V and 1.26 V, respectively. The charge and discharge stages lasted 13.42 h and 12.42 h, respectively. The system using Electrolyte B showed charge-discharge efficiency of 95.6% and mean charge and discharge voltage values of 1.56 V and 1.266 V, respectively. In this case, the charge and discharge stages lasted 12.65 h and 12.09 h, respectively. The system using Electrolyte C showed a charge-discharge efficiency of 77.2% and mean charge and discharge voltages of 1.59 V and 1.21 V, respectively. The charge and discharge stages with Electrolyte C lasted 7.19 h and 5.52 h, respectively.

Fig. 6. Charge-discharge cell voltage profile as function of normalized time by varying the electrolyte preparation method.

Fig. 6 shows the plots of cell voltage versus the normalized charge-discharge time, here defined as t/t_{max} (t_{max} = time of an complete charge-discharge time) for Electrolytes A-C. The theoretical energy density of the analysed electrolyte corresponded corresponds to 37.8 Wh L⁻¹ for Electrolytes A and B, with Electrolyte C energy density being ca. 30.0 Wh L⁻¹. Table 4 summarizes cycle performance parameters of flow cell using Electrolytes A-C.

The lower performance exhibited by Electrolyte C compared to Electrolyte A and B, is mainly due to its lower value of total vanadium and chloride concentrations. In fact, the reduced electrolyte electrical conductivity also negatively influences the battery performance.

Table 45

The lower performance exhibited by Electrolyte C compared to Electrolytes A and B, is reasonably due to its lower value of total vanadium and chloride concentrations. In fact, the reduced electrolyte electrical conductivity adversely affects also the battery performance. Indeed as supported by EIS measurement the internal resistance of cell using Electrolyte C results the highest.

Table 6 shows a comparison of the performance of the VRF cells using 2.5 M and 3.0 M vanadium mixed sulphate-chloride electrolytes with that using 1.6 M vanadium sulphate electrolyte [22]. It is apparent that Electrolytes A and B (entries 1 and 2, respectively) showed energy efficiencies comparable to mixed acid literature systems reported in entries 4 and 5, considering that the experimental conditions used for the determination of the VRF cell were different. It is interesting to note that the pure sulphate system (entry 6) shows an energy efficiency comparable to that of the mixed acid systems, but having a lower total V concentration. Electrolyte C, which contains a lower V concentration in the presence of a mixed acid system, expectedly showed the lowest energy efficiency (77 %, entry 3).

Table 6

3.7. LCA analysis

LCA analysis has its beginning in 1960', as the limitations of raw materials and energy resources have aroused interest in research which has developed of methods to accounting for the flows of matter and energy. From then on, the

International Organization for Standardization (ISO) has recognized the validity of the LCA model (proposed by the Society of Environmental Toxicology and Chemistry) through the 14040 series of standards, defining LCA as a tool for "compilation and evaluation throughout the life cycle of the flows in and out, and the potential environmental impacts of a product system". The assessment, in the analysed study, includes the processes of the life cycle from the "cuddle cradle to the gate". It includes the extraction and processing of raw materials and product manufacturing. The assessment of the life-cycle is structured as an input-output matrix listing all the factors of impact on the environment on the rows and all phases and sub-phases that concur to form the life cycle of a product or of a service on the columns. In this paper, LCA was used to compare provide a benchmark of the three Electrolytes electrolytes A-C from the an environmental point of view. The three electrolytes A,B and C were prepared through different procedures but intended for the same use even though synthesised using different procedures.

The eEcopoints for a series number of environmental impact categories were calculated for each electrolyte using the ReCiPe method [2433] as shown in Fig. 7. Contributions to the environmental impact are given by: human health particulate matter formation, human health climate change, resources fossil depletion, ecosystem quality climate change. It is apparent evident in Fig. 7 that the three methods for the synthesis methods of Electrolytes A-C create comparable impacts of the same order of magnitude from the qualitative point of view, as being the typologies of environmental concern are tied the same chemical species the same for all of the electrolytes. Nevertheless, In general, contributions on the environmental impact are created by: human health particulate matter formation, human health climate change, resources fossil depletion, ecosystem quality climate change. On the other hand, a significant differences in within each impact can be appreciated comparing the each Ecopoints calculated for each electrolyte.

Fig. 7. Characterization-Comparison of levels of environmental impact (for each impact category) of the Electrolytes A-C. ReCiPe method (I/A). Amounts in Ecopoints (Ecopoint = one thousandth of the yearly environmental load of an average citizen of Europe).

The radar graph shown in Fig. 8 reports the Ecopoints of the three endpoints considered in the ReCiPe method (i.e. damage to human health, damage to the ecosystems), and damage to the availability of resources) along with the sum of the three Ecopoints (total). Electrolyte C is the one which shows the lowest impact, while Electrolyte B is endowed with the highest impact. The biggest damage on the environment is associated to the use of fossil sources. In fact, they act on the climate changes and on the formation of particulate in the air creating, as a consequence, a damage on the ecosystem and on the human health.

Fig. 8. Assessing environmental damage.- Comparison of environmental damage: damage to health human damage to the ecosystem and to the depletion of resources, generated by the methods of synthesis of electrolytes Electrolytes A-C. Recipe method Endpoint (I/A). Amounts in Ecopoints.

4. Conclusions

The This paper presents discloses benchmarking results of on the electrochemical performances and sustainability features benchmark amongst of three different preparation methods of a mixed-acid working vanadium-based -electrolytes for

VRFB systems. Electrolyte A was prepared by mere mixing of suitable vanadium precursors; , Electrolyte B was synthesized by the chemical reduction of V2O5 by oxalic acid and while Electrolyte C was prepared using an electrochemical reduction of V2O5 in a home-made "H-shaped" electrolysis cell.

The Electrolytes A-C allowed the battery to operate stably and more efficiently, in a wider range of temperature with respect to a conventional pure sulphate electrolyte.

Methods for Electrolytes A and B resulted in excellent electrolytes in terms of gave very satisfactory electrochemical performance and their preparation. These latter methods guarantee ensured a complete full control on of preparation process allowing to meeting the target required in terms of total vanadium and chloride concentration as well as electrolyte properties and performances. The method adopted to synthesise Electrolyte C was useful to convert vanadium pentoxide in VRFB working electrolyte; nevertheless it need to be improved to reach the performance targets obtained with the other two methods.

Method forThe synthesis of Electrolyte A resulted in a very simple implementable process, but it can hardly be industrialised, due to showed a very poor industrial relevance because of the very high cost of vanadium precursors. .M Method adopted for Electrolyte B could can be easily be easily implemented as an industrial process, as it starts from the readily available for mixed acid vanadium electrolyte preparation, because it was based on the reduction of relatively inexpensive V2O5. The use need of a reducing agent - in this case, (oxalic acid) for Electrolyte B- resulted results in a higher electrolyte cost production (to date the reference price of 99.5% oxalic acid corresponds to 0.742\$/kg the quotation of 99.6% oxalic acid in December 2010 corresponding to about 0.849\$/kg [2941]), and lower process environmental sustainability with respect to the case of Electrolyte method C., in In fact, according to reaction (1), approximately 0.7 ton. of oxalic acid are required to reduce 1.0 ton. of vanadium pentoxide and at the same time approximately 0.5 ton. of carbon dioxide were are produced. Furthermore, this latterthe preparation of Electrolyte B process requires the use of supplementary energy an additional step to produce a VRFB working electrolyte, requiringnecessary to achieve the desired 1:1 V³⁺/V^{O2+} molar ratio the use of supplementary energy.

Electrolytes A and B showed energy efficiencies comparable to mixed sulphate-chloride literature systems while Electrolyte C showed lower performance Electrolyte C is endowed with the lowest energy efficiency, due to its relatively low V concentration in the presence of chloride ions.

LCA analysis identifies the preparation of Electrolyte C as the best methodology in terms of environmental sustainability, showing potential interest in the methodology. Future efforts should be devoted to synthesize a mixed acid electrolyte using methodology C, but with a final V concentration higher than 2.0 M.

mainly related to dilution due to water transport through the membrane during its preparation, resulting in lower energy density. Even if in terms of electrochemical features Electrolyte C showed the best redox reversibility of V^{O2+}/V^{O2+} and a faster charge transfer reaction kinetic at the electrolyte/electrode interface on carbon, felt respect to Electrolytes A-B. This behaviour was mainly related to the design and operative condition and configuration of experimental facilities employed. The "H-shape" electrolysis-cell needs to be optimized in design and operation in order to reduce the electrical resistance, and improve the mixing efficiency.

By improving design, operative condition and configuration of “H-shape” electrolysis cell, the V205 fully electrolyte reduction process, i.e. method C, should guarantee the production of VRFB a mixed acid working electrolyte with excellent performance, while ensuring the process cost effectiveness, required for the implementation of industrially relevant process.

Still there is room for improvements, considering the geographical origin of the raw materials (which should be as closer as possible to the production site) and to the type of energy mix used, which should be obtained by renewable rather than by fossil sources.

Acknowledgements

The experimental procedure at the basis of this paper has been partially funded within the frame of the project “GEI5 - Green Energy Island: Stand alone hybrid system for generation and storage of renewable energy”, granted by Duferco Engineering SpA.. This paper has been developed under the moral patronage of the ‘SOSTENERE’ Group of the Italian Association of Mechanical Technologist (AITEM).

References

- [1] Thaller LH. Redox flow cell energy storage systems. 1979.
- [2] Giner J, Swette L, Cahill K. Screening of redox couples and electrode materials. 1976.
- [3] Beaudin M, Zareipour H, Schellenberg A, Rosehart W. Energy storage for mitigating the variability of renewable electricity sources: An updated review. *Energy Sustain Dev* 2010;14:302–14. doi:10.1016/j.esd.2010.09.007.
- [4] Chen H, Cong TN, Yang W, Tan C, Li Y, Ding Y. Progress in electrical energy storage system: A critical review. *Prog Nat Sci* 2009;19:291–312. doi:10.1016/j.pnsc.2008.07.014.
- [5] Salameh Z. Chapter 4 - Energy Storage. In: Salameh Z, editor. *Renew. Energy Syst. Des.*, Boston: Academic Press; 2014, p. 201–98.
- [6] Skyllas-Kazacos M, Kazacos G, Poon G, Verseema H. Recent advances with UNSW vanadium-based redox flow batteries. *Int J Energy Res* 2010;34:182–9. doi:10.1002/er.1658.
- [7] Soloveichik GL. Flow Batteries: Current Status and Trends. *Chem Rev* 2015;115:11533–58. doi:10.1021/cr500720t.
- [8] Cunha Á, Martins J, Rodrigues N, Brito FP. Vanadium redox flow batteries: a technology review. *Int J Energy Res* 2015;39:889–918. doi:10.1002/er.3260.
- [9] Ontiveros LJ, Mercado PE. Modeling of a Vanadium Redox Flow Battery for power system dynamic studies. *Int J Hydrog Energy* 2014;39:8720–7. doi:10.1016/j.ijhydene.2013.12.042.
- [10] Baumann L, Boggasch E. Experimental assessment of hydrogen systems and vanadium-redox-flow-batteries for increasing the self-consumption of photovoltaic energy in buildings. *Int J Hydrog Energy* 2016;41:740–51. doi:10.1016/j.ijhydene.2015.11.109.
- [11] Ibrahim H, Ilinca A, Perron J. Energy storage systems—Characteristics and comparisons. *Renew Sustain Energy Rev* 2008;12:1221–50. doi:10.1016/j.rser.2007.01.023.
- [912] Skyllas-Kazacos M, Chakrabarti MH, Hajimolana SA, Mjalli FS, Saleem M. Progress in Flow Battery Research and Development. *J Electrochem Soc* 2011;158:R55. doi:10.1149/1.3599565.
- [130] Skyllas-Kazacos M, Kasherman D, Hong DR, Kazacos M. Characteristics and performance of 1 kW UNSW vanadium redox battery. *J Power Sources* 1991;35:399–404. doi:10.1016/0378-7753(91)80058-6.

- [14] Hadjipaschalis I, Poullikkas A, Efthimiou V. Overview of current and future energy storage technologies for electric power applications. *Renew Sustain Energy Rev* 2009;13:1513–22. doi:10.1016/j.rser.2008.09.028.
- [151] Parasuraman A, Lim TM, Menictas C, Skyllas-Kazacos M. Review of material research and development for vanadium redox flow battery applications. *Electrochimica Acta* 2013;101:27–40. doi:10.1016/j.electacta.2012.09.067.
- [16] Cunha Á, Brito FP, Martins J, Rodrigues N, Monteiro V, Afonso JL, et al. Assessment of the use of vanadium redox flow batteries for energy storage and fast charging of electric vehicles in gas stations. *Energy* n.d. doi:10.1016/j.energy.2016.02.118.
- [172] Ding C, Zhang H, Li X, Liu T, Xing F. Vanadium Flow Battery for Energy Storage: Prospects and Challenges. *J Phys Chem Lett* 2013;4:1281–94. doi:10.1021/jz4001032.
- [18] Wang Y, Wang S, Xiao M, Han D, Meng Y. Preparation and characterization of a novel layer-by-layer porous composite membrane for vanadium redox flow battery (VRB) applications. *Int J Hydrog Energy* 2014;39:16088–95. doi:10.1016/j.ijhydene.2014.02.100.
- [19] Wang Y, Wang S, Xiao M, Song S, Han D, Hickner MA, et al. Amphoteric ion exchange membrane synthesized by direct polymerization for vanadium redox flow battery application. *Int J Hydrog Energy* 2014;39:16123–31. doi:10.1016/j.ijhydene.2014.04.049.
- [20] Vynnycky M. Analysis of a model for the operation of a vanadium redox battery. *Energy* 2011;36:2242–56. doi:10.1016/j.energy.2010.03.060.
- [1321] Kim S, Thomsen E, Xia G, Nie Z, Bao J, Recknagle K, et al. 1 kW/1 kWh advanced vanadium redox flow battery utilizing mixed acid electrolytes. *J Power Sources* 2013;237:300–9. doi:10.1016/j.jpowsour.2013.02.045.
- [1422] Li L, Kim S, Wang W, Vijayakumar M, Nie Z, Chen B, et al. A Stable Vanadium Redox-Flow Battery with High Energy Density for Large-Scale Energy Storage. *Adv Energy Mater* 2011;1:394–400. doi:10.1002/aenm.201100008.
- [1523] Kim S, Vijayakumar M, Wang W, Zhang J, Chen B, Nie Z, et al. Chloride supporting electrolytes for all-vanadium redox flow batteries. *Phys Chem Chem Phys* 2011;13:18186. doi:10.1039/c1cp22638j.
- [1624] Fang B, Iwasa S, Wei Y, Arai T, Kumagai M. A study of the Ce(III)/Ce(IV) redox couple for redox flow battery application. *Electrochimica Acta* 2002;47:3971–6. doi:10.1016/S0013-4686(02)00370-5.
- [1725] Huang F, Zhao Q, Luo C, Wang G, Yan K, Luo D. Influence of Cr³⁺ concentration on the electrochemical behavior of the anolyte for vanadium redox flow batteries. *Chin Sci Bull* 2012;57:4237–43. doi:10.1007/s11434-012-5302-0.
- [1826] Li S, Huang K, Liu S, Fang D, Wu X, Lu D, et al. Effect of organic additives on positive electrolyte for vanadium redox battery. *Electrochimica Acta* 2011;56:5483–7. doi:10.1016/j.electacta.2011.03.048.
- [1927] Peng S, Wang N, Gao C, Lei Y, Liang X, Liu S, et al. Stability of Positive Electrolyte Containing Trishydroxymethyl Aminomethane Additive for Vanadium Redox Flow Battery. *Int J Electrochem Sci* 2012;7:4388–96.
- [28] Rydh CJ. Environmental assessment of vanadium redox and lead-acid batteries for stationary energy storage. *J Power Sources* 1999;80:21–9. doi:10.1016/S0378-7753(98)00249-3.
- [2029] ISO I. 14040: Environmental management–life cycle assessment–principles

and framework. Lond Br Stand Inst 2006.

[2130] ISO I. 14044: environmental management–life cycle assessment–requirements and guidelines. Int Organ Stand 2006.

[2231] Azapagic A, Perdan S. Indicators of sustainable development for industry: a general framework. Process Saf Environ Prot 2000;78:243–61.

[2332] UNEP S, Initiative LC. Life Cycle Management–A Business Guide to Sustainability. U N Environ Programme Paris Fr 2007.

[2433] Goedkoop M, Heijungs R, Huijbregts M, De Schryvera A, Struijs J, Van Zelm R, 2009 - ReCiPe 2008: A life cycle impact assessment method which comprises harmonised category indicators at the midpoint and the endpoint level. VROM–Ruimte en Milieu, Ministerie van Volkshuisvesting, Ruimtelijke Ordening en Milieubeheer, www.lcia-recipe.net.

[2534] Guinée JB. Handbook on life cycle assessment operational guide to the ISO standards. Int J Life Cycle Assess 2002;7:311–3.

[2635] United Nations, editor. Evaluation of environmental impacts in life cycle assessment: meeting report, Brussels, 29 - 30 November 1998, and Brighton, 25 - 26 May 2000. Paris: 2003.

[36] Thompson M, Ellis R, Wildavsky A. Cultural Theory. Boulder: Westview Press; 1990.

[2737] Mastroilli P, Rizzuti A, Dassisti M, Cozzolino G, Chimienti M. Investigation on a new mixed acid based support electrolyte for a Vanadium Redox Flow Battery. vol. 1, Bari, Italy: Politecnico di Bari ; Gangemi; 2014, p. 141–6.

[38] Zhang J, Li L, Nie Z, Chen B, Vijayakumar M, Kim S, et al. Effects of additives on the stability of electrolytes for all-vanadium redox flow batteries. J Appl Electrochem 2011;41:1215–21. doi:10.1007/s10800-011-0312-1.

[2839] Wang WH, Wang XD. Investigation of Ir-modified carbon felt as the positive electrode of an all-vanadium redox flow battery. Electrochimica Acta 2007;52:6755–62. doi:10.1016/j.electacta.2007.04.121.

[2940] Li W, Liu J, Yan C. Graphite-graphite oxide composite electrode for vanadium redox flow battery. Electrochimica Acta 2011;56:5290–4. doi:10.1016/j.electacta.2011.02.083.

[3041]

[http://www.molbase.com/en/search.html?search_keyword=\[oxalic%20acid\]&gclid=CLOV_jer8wCFWMq0wodOGsLBw](http://www.molbase.com/en/search.html?search_keyword=[oxalic%20acid]&gclid=CLOV_jer8wCFWMq0wodOGsLBw)

<http://www.businesswire.com/news/home/20110111006011/en/Research-Markets-Chinas-Oxalic-Acid-Industry-2010-2012#.VM95CWig8jw> n.d.